# Hybrid silicon slotted photonic crystal waveguides: how does third order nonlinear performance scale with slow light?

**Junfei Xia,[1] Samuel Serna,[1,2] Weiwei Zhang,[1] Laurent Vivien,[1] and Éric Cassan[1,*]**

[1]*Centre de Nanosciences et de Nanotechnologies, UMR 9001 (CNRS/Université Paris-Sud), Université Paris-Saclay, 91405 Orsay, France*
[2]*Laboratoire Charles Fabry, Institut d'Optique, CNRS, Université Paris-Sud, 2 Avenue Augustin Fresnel, 91127 Palaiseau Cedex, France*
**Corresponding author: eric.cassan@u-psud.fr*

Received July 12, 2016; revised September 22, 2016; accepted September 22, 2016; posted September 28, 2016 (Doc. ID 270353); published October 20, 2016

We investigate in this paper the influence of slow light on the balance between the Kerr and two-photon absorption (TPA) processes in silicon slotted hybrid nonlinear waveguides. Three typical silicon photonic waveguide geometries are studied to estimate the influence of the light slow-down factor on the mode field overlap with the silicon region, as well as on the complex effective nonlinear susceptibility. It is found that slotted photonic crystal modes tend to focalize in their hollow core with increasing group index ($n_G$) values. Considering a hybrid integration of nonlinear polymers in such slotted waveguides, a relative decrease of the TPA process by more factor of 2 is predicted from $n_G = 10$ to $n_G = 50$. As a whole, this work shows that the relative influence of TPA decreases for slotted waveguides operating in the slow light regime, making them a suitable platform for third-order nonlinear optics. © 2016 Chinese Laser Press

*OCIS codes:* (230.5298) Photonic crystals; (130.5296) Photonic crystal waveguides; (230.4320) Nonlinear optical devices; (190.4390) Nonlinear optics, integrated optics.
http://dx.doi.org/10.1364/PRJ.4.000257

## 1. INTRODUCTION AND MOTIVATIONS

Silicon photonics based on the silicon-on-insulator photonics platform has shown tremendous progress in the last years. The path to miniaturization of optical components and the realization of chips made of integrated optical and electronic functions is now assessed by concrete demonstrations [1]. In this perspective, on-chip nonlinear optical effects offer another dimension with the promise of all-optical signal processing capabilities enabling ultra-high-speed data conversion and massively parallel data processing. Among the explored nonlinear functions, optical parametric amplification, supercontinuum generation, all-optical switching, second- and third-harmonic generation, and frequency comb generation have been actively investigated [1–5]. Due its lattice symmetry, (unstrained) silicon itself does not present second order nonlinearity. On the contrary, third-order effects are strong in silicon ($n_2 \approx 6.10^{-18}$ m$^2$ W$^{-1}$ at $\lambda = 1.55$ μm). Yet Kerr and other $\chi^{(3)}$ nonlinear effects are directly spoiled by free carriers generated by two-photon absorption (TPA) [3,6]. One possible solution to alleviate this drawback at telecommunication wavelengths is the use of silicon hollow core slotted waveguides, while filling their core region with active nonlinear materials [7]. In order to further reinforce light–matter interactions, slot photonic crystal waveguides (SPCWs) can be considered, namely, by relying on slow light effects [8–10]. Although the use of slotted waveguides brings improvement to the aforementioned free carrier issue, it does not solve entirely the free carrier penalty as only 25%–40% of the propagating optical mode dielectric energy is usually confined in the low index soft material filling the slot. As a consequence, TPA in silicon, which directly depends on the optical mode spreading outside the slot, cannot be entirely removed.

For a standard slot waveguide, the spatial overlap between the two silicon rails and the optical mode profile is invariant according to the light propagation axis. Previous results dedicated to standard slow light W1 waveguides have shown on the contrary that the gap-guided mode field profile tends to spread in silicon when approaching the bandgap, thus by increasing the slow-down factor [11]. In this context, the present paper proposes an investigation of the slow light effects on the third-order effective optical nonlinearities of hybrid silicon SPCW.

Slow-light enhancement of the third-order nonlinearity is the underlying motivation of this approach. In a more quantitative fashion, it is known from previous works that the effective waveguide nonlinear susceptibility $\chi^{(3)}$ scales as $n_G^2$, where $n_G$ is the light group velocity of the photonic crystal waveguide (PCW) mode [12]. This scaling behavior opens the path to reach nonlinear optical effects, including self-phase and cross-phase modulations as well as four wave mixing processes, at low optical pumping powers. Considering reasonable slow-down factors typically corresponding to $n_G = 20 - 40$, this approach can lead to spectacular effective nonlinear parameter $\gamma$ values of a few thousands of W$^{-1}$ m$^{-1}$ in silicon PCWs [4]. Further considerations indicate that both Re($\gamma$) and Im($\gamma$) scale as $n_G^2$, meaning that increased Kerr effect is accompanied by an increase in TPA. Considering the TPA figure of merit (FOM) introduced in

 © 2016 Chinese Laser Press

previous works as $\mathrm{FOM_{TPA}} = -\mathrm{Re}(\gamma)/4\pi\,\mathrm{Im}(\gamma)$ [3], it turns out that $\mathrm{FOM_{TPA}}$ is supposed to be slow light invariant. In other words, although a spectacular increase of $\mathrm{Re}(\gamma)$ is obtained, the true net benefit of slow light with respect to the third-order nonlinearities completely vanishes to zero. Mode field spreading in silicon as a function of increasing $n_G$ values is even an issue with respect to TPA minimization [11]. Even though this is true when considering a single nonlinear material, further research is required to study hybrid waveguides.

## 2. RESULTS AND DISCUSSION

In order to investigate this question, we consider here several photonic crystal geometries, including nonslotted and slotted waveguides. We calculate for each their dispersion and nonlinear properties as a function of the light group index. Typical silicon photonic waveguide parameters are considered, so that results obtained can be estimated as general trends for this photonic platform. A lattice constant $a = 400$ nm and a silicon thin film of 260 nm height on a buried box of 2 μm have been first adopted. Standard linear refraction index values of 3.48 and 1.44 at $\lambda = 1.55$ μm are retained for Si and $SiO_2$, respectively, with a Kerr index $n_2 = 6 \times 10^{-18}$ m$^2$/W and a TPA coefficient $\beta_{\mathrm{TPA}} = 1.0 \times 10^{-11}$ m/W for silicon at this wavelength. The present study is driven in regard with doped nonlinear polymers (NP), whose base refractive index is very close to 1.50, some of them having interesting nonlinear optical properties at telecommunication wavelengths [13,14]. A top cladding material with a linear index of 1.5, a Kerr index $n_2 = 2 \times 10^{-17}$ m$^2$/W, and a TPA coefficient $\beta_{\mathrm{TPA}} = 2.6 \times 10^{-12}$ m/W are considered as a typical situation of a strongly nonlinear soft material filling the slot and holes of the SPCW [15]. Recasting these values in terms of the Kerr/TPA FOM of the two materials, one gets $\mathrm{FOM_{Si}} \approx 0.38$ and $\mathrm{FOM_{NP}} \approx 5.0$ at $\lambda = 1.55$ μm, respectively. Before any quantitative estimation of the impact of TPA on the hybrid waveguide slot waveguide, an intermediate value of the waveguide $\mathrm{FOM_{TPA}}$ can thus be predicted, that is, ranging between 0.38 and 5.0. According to previous results, an effective waveguide $\mathrm{FOM_{TPA}}$ ideally well above 1.0 is desirable for on-chip all-optical data processing [1]. These different values are given here to serve in the analysis of the results presented hereafter in the article.

The three investigated geometries are made of a W1 PCW (W1-PCW), a narrow slot SPCW (NS-PCW), and a wide slot PCW (WS-PCW), as shown in Fig. 1. Choosing significantly different values for the slot widths of the NS-PCW ($W_{\mathrm{slot}} = 100$ nm) and the WS-PCW ($W_{\mathrm{slot}} = 175$ nm) leads to the possibility of exploiting the so-called "W1-like mode" and "true-slot mode" of SPCWs while ensuring large enough slots to avoid fabrication issues and guarantee proper filling [7]. With respect to the standard situation of the W1-PCW made of identical holes of 105 nm radius and width of $\sqrt{3}a$, the width of the NS-PCW and WS-PCW is enlarged to $1.25\sqrt{3}a$, following previous guidelines [9,10]. The radius values of the lattice holes of the slotted waveguides are also adjusted to $r_1 = 135$ nm and $r = 120$ nm for the NS-PCW and $r_1 = 125$ nm and $r = 115$ nm for the WS-PCW in order to prepare single-mode propagation and nearly mid-gap conditions for each investigated $E_y$-even mode. All calculations have been conducted by using the three-dimensional (3D) plane wave expansion (PWE) method [16] and postprocessing of the obtained data.

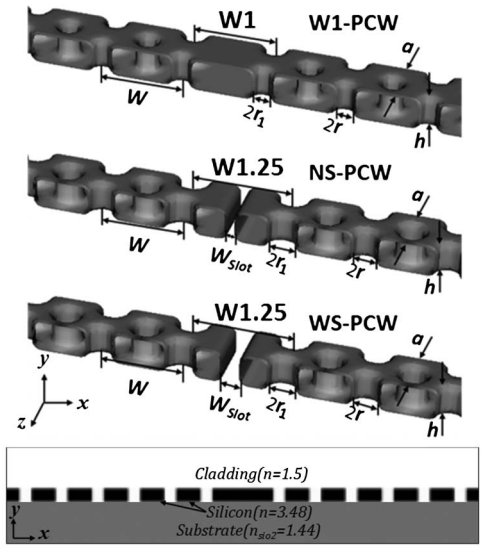


Fig. 1. Schematic views of the investigated PCW geometries (W1-PCW, NS-PCW and WS-PCW). $a = 400$ nm, $h = 260$ nm. Other parameters are specified in the text.

Figure 2 shows the three obtained dispersion diagrams. A first outcome is that negative and positive frequency-band slopes are obtained for the W1-PCW, NS-PCW, and WS-PCW, as expected. We also observe that a large fraction of each eigenband is situated below the top cladding light line ($n_{\mathrm{clad}} = 1.50$). This fact is an important prerequisite for the viability of the investigated hybrid photonic platform based on nonmembrane hollow core silicon PCWs filled by nonlinear soft materials. Consistently with the main objective of the present study, namely the investigation of the effect of slow light on the nonlinear properties of the chosen hybrid waveguides, the dispersion properties of the three waveguides have been then investigated. More specifically, the mode group index ($n_G$) and group velocity dispersion (GVD) coefficient ($\beta_2$) have been calculated from the 3D-PWE calculation results. The results are depicted in Fig. 3.

Group index ($n_G$) values below 50 are plotted here as it is known from previous works that extrinsic optical losses in PCWs dramatically increase above that value [17]. The three waveguide geometries have been deliberately chosen here without any dispersion-engineering strategy, so further optimization of GVD remains possible. As waited, strong dispersion values ($\beta_2 \gg 1$ ps$^2$/cm) can thus be observed as soon as $n_G > 10 - 15$. More interestingly, a striking point can be inferred from the insets of Figs. 3(a), 3(b), and 3(c), which depict the three mode profiles for increasing group index values.

As visible in Fig. 3(a), the W1-PCW mode tail spreading tends to increase for increasing light slow-down factors (from $A_1$ to $A_5$), consistent with previously reported results. When exploiting the W1-like mode (in NS-PCW), there is also a field spreading effect of the tails of the guided mode with a simultaneous increase of the energy intensity in the center of the waveguide [from $B_1$ to $B_5$; see Fig. 3(b)]. In the case of the WS-PCW, the true slot mode is characterized on the contrary by a mode profile compression of the mode tails [from $C_1$ to $C_5$; Fig. 3(c)], which further reinforces the light–matter

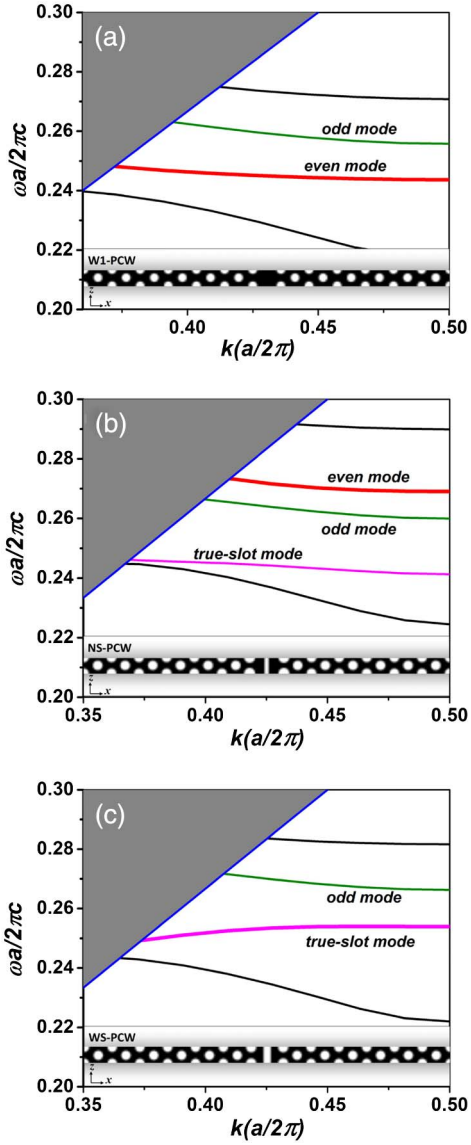


Fig. 2. Dispersion curves of the three PCWs described in Fig. 1: (a) W1-PCW, (b) NS-PCW, and (c) WS-PCW.

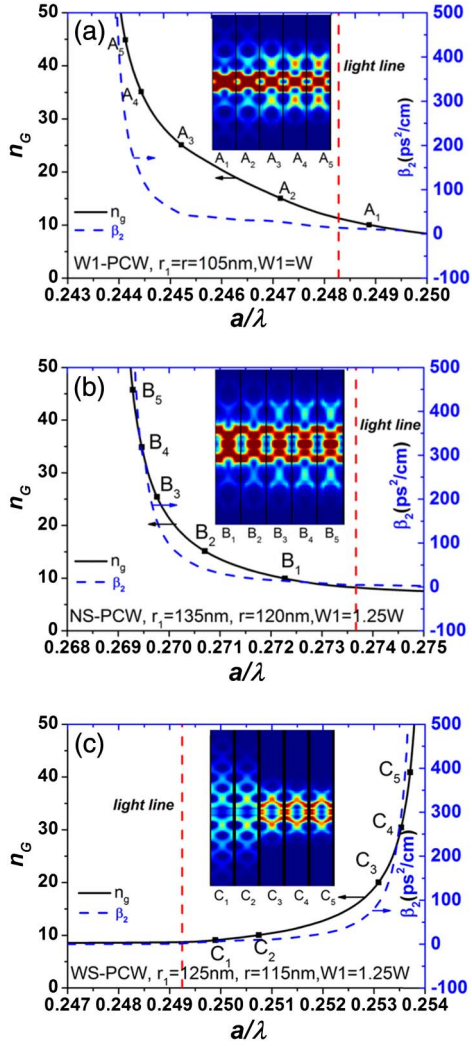


Fig. 3. Waveguide mode group index ($n_G$) and dispersion coefficient ($\beta_2$) of the three investigated PCWs (see Fig. 1): (a) W1-PCW, (b) NS-PCW, and (c) WS-PCW.

interaction with the nonlinear material filling the slot in the center.

Slow light arises due to the interaction between forward and backward propagating wave components. In the case of slotted PCW waveguides, this effect is combined with the slot discontinuity of the material permittivity that is responsible for the electric field confinement into the low index slot region. From the performed numerical investigations, we infer that the combined slow light and slot effects are responsible for an increase of light power into the slot in the slow light regime.

In order to investigate the consequences of these qualitative trends on the third-order nonlinear optical properties of the three waveguides, several nonlinear parameters have been calculated for each. Similar approaches as those conducted in [3] and [18,19] for silicon wire and W1 waveguides, respectively, have been considered. As stated in these works, mode field spreading in the silicon region can be responsible for the generation of carriers by the TPA process, which in turn are responsible for the free-carrier dispersion and absorption effects. These different mechanisms should be introduced in the nonlinear Schrödinger equation (NLSE) that can be solved, for instance, by the split-step method [3]. Yet, in order to investigate the amount of free carriers, estimation of only one parameter is necessary as all terms of the NLSE depending on free carriers scale with them:

$$\kappa(z) = \frac{a n_{\mathrm{Si}}^2 \int_{S_{\mathrm{si}}} |\mathbf{e}(\mathbf{r})|^2 \mathrm{d}S}{\int_{V_{\mathrm{cell}}} \frac{\partial}{\partial \omega}(\omega n_c^2) |\mathbf{e}(\mathbf{r})|^2 \mathrm{d}V}, \tag{1a}$$

$$\langle \kappa(z) \rangle = \frac{1}{a} \int_0^a \kappa(\xi) \mathrm{d}\xi, \tag{1b}$$

where $V_{\mathrm{cell}}$ is the volume of the supercell for the calculation, $n_c$ is the refractive index, and $S_{\mathrm{si}}$ is the effective area in the cross section ($xy$ plane) [3,18,19]. The $\langle \kappa(z) \rangle$ coefficient characterizes in fact the overlap between the optical mode and the silicon region. This parameter ($0 < \langle \kappa(z) \rangle < 1$) is of direct interest for the quantitative estimation of the free carrier effects depending on the slow-down factor.

We also retained another important metric, the effective waveguide third-order susceptibility first calculated, at one specific $z$ point over the waveguide lattice period Eq. (2a) [18,19]:

$$\Gamma(z) = \frac{a^4 \int_{S_{\mathrm{nl}}} \mathbf{e}(\mathbf{r})^* \cdot \chi^{(3)}(\mathbf{r}) \vdots \mathbf{e}(\mathbf{r})\mathbf{e}(\mathbf{r})\mathbf{e}^*(\mathbf{r}) \mathrm{d}S}{\left(\int_{V_{\mathrm{cell}}} \frac{\partial}{\partial \omega}(\omega n_c^2)|\mathbf{e}(\mathbf{r})|^2 \mathrm{d}V\right)^2}, \tag{2a}$$

$$\langle \Gamma \rangle_z = \frac{1}{a}\int_0^a \Gamma(\xi)\mathrm{d}\xi, \tag{2b}$$

where $S_{\mathrm{nl}}$ corresponds to the optical nonlinear region.

Similarly, averaging this quantity over one lattice period leads to $\langle \Gamma(z) \rangle$, Eq. (2b) that is, to the effective waveguide nonlinear susceptibility. These two parameters have been calculated in the three waveguide configurations described above, namely, by considering the W1 and two slotted hybrid silicon PCWs. In the three cases, nonlinearity comes from both silicon and the nonlinear material filling the holes and the slot. For each material, estimation of $\chi^{(3)\prime}$ and $\chi^{(3)\prime\prime}$ has been done from the $n_2$ and $\beta_{\mathrm{TPA}}$ parameters, as follows [3]:

$$\frac{\omega}{c} n_2 + \frac{i}{2}\beta_{\mathrm{TPA}} = \frac{3\omega}{4\varepsilon_0 c^2 n^2}\chi^{(3)}_{\mathrm{eff}}. \tag{3}$$

The integration over space in Eq. (2) was done over the full photonic crystal lattice cell, that is, by considering both Si and NP as nonlinear materials, each having a complex nonlinear susceptibility. The Kerr/TPA FOM describing the balance between index modulation and free-carrier effects was then finally calculated by considering the classical relationship $\mathrm{FOM_{TPA}} = -\mathrm{Re}(\Gamma)/4\pi\,\mathrm{Im}(\Gamma)$. Additionally, the waveguide nonlinear parameter $\gamma$ was calculated as $\gamma = 3\omega\Gamma n_G^2/4\varepsilon_0 a^2$ [17]. Obviously, whatever the fast/slow light regime be (e.g., whatever the $n_G$ value is), $\mathrm{FOM_{TPA}}$ can be indifferently defined from $\gamma$ or $\Gamma$, namely, as $\mathrm{FOM_{TPA}} = -\mathrm{Re}(\gamma)/4\pi\,\mathrm{Im}(\gamma)$ or $\mathrm{FOM_{TPA}} = -\mathrm{Re}(\Gamma)/4\pi\,\mathrm{Im}(\Gamma)$. We come back here to the point mentioned at the beginning of the article: to the first order, $\mathrm{FOM_{TPA}}$ is $n_G$-invariant. We yet arrive here to a more quantitative result: $\mathrm{FOM_{TPA}}$ depends in fact on $\langle \Gamma(z) \rangle$, as the mode field spreading in space is modified by the light slowing-down factor (see Fig. 3).

The extent of slow light reinforcement or minimization of free-carrier-induced-TPA can be investigated by calculating the $\langle \kappa \rangle$, $\langle \gamma \rangle$, $\langle \Gamma \rangle$, and $\mathrm{FOM_{TPA}}$ parameters as a function of $n_G$. The related results are shown in Figs. 4 and 5. Figure 4(a) by itself brings a first interesting quantitative result: the mode field/silicon overlap in the W1 waveguide is extremely large (>90%) and is nearly constant (although a very small decrease is appreciable), while $\langle \kappa(z) \rangle$ decreases for increasing slow-down factors in SPCWs. This overlap drops further (by around 20%) for the wide SPCW that exploits the so-called even true slot mode [see Fig. 2(c)].

To further analyze the waveguide properties, we plot in Fig. 4(b) Re(Γ) and Im(Γ) as a function of $n_G$ (with a double $y$ axis to manage two different scales). The W1-PCW (solid and dashed black lines) is characterized by a slight decrease of both quantities for increasing $n_G$ values, so a small evolution is predicted for this geometry. Interestingly, we observe that the NS-PCW (red lines) presents a small decrease of

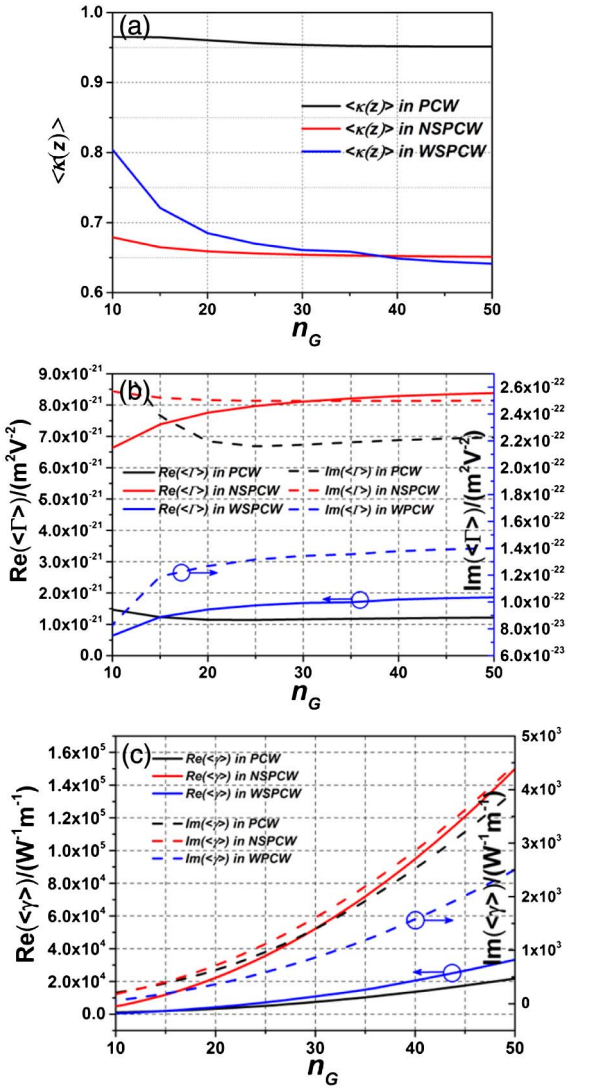


Fig. 4. Nonlinear properties parameters versus group indices: (a) mode field/silicon overlap factor, (b) effective nonlinear susceptibility in terms of real and imaginary parts, (c) nonlinear waveguide parameter (real and imaginary parts).

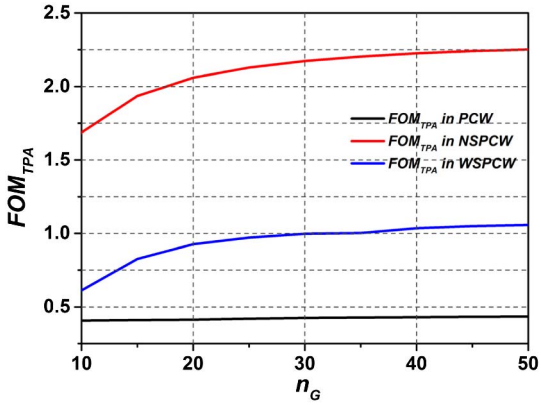


Fig. 5. $\mathrm{FOM_{TPA}}$ in the three investigated structures. Black, red, and blue curves represent the parameters in W1-PCW, NS-PCW, and WS-PCW, respectively.

Im(Γ) and simultaneously an increase of Re(Γ). This means that the in-slot mode field refocusing effect efficiently contributes to the increase of the effective $\mathrm{Re}(\chi^{(3)})$ while minimizing the silicon TPA contribution in silicon. As far as it is concerned, the WS-PCW case (blue lines) is characterized by an increase of both Re(Γ) and Im(Γ). A careful look on the two axis scales shows in fact that the Re(Γ) increase is higher than the Im(Γ) one.

Figure 4(c) shows that the combined effect of $n_G^2$ and $\langle\Gamma(z)\rangle(n_G)$ is dominated by the former one, as predicted. More interestingly, we observe that group index values around 15–20 are sufficient to lead to Re($\gamma$) values of 5000–20000 $\mathrm{W^{-1}\,m^{-1}}$ in hybrid silicon SPCWs, that is, at least 50 times larger than those obtained for typical silicon slot waveguides [7].

The final firm information regarding the effect of slow waves on the Kerr/TPA balance in the investigated standard and slotted PCW is depicted in Fig. 5. We plot here $\mathrm{FOM_{TPA}}$ of the three waveguides as a function of $n_G$. As visible, $\mathrm{FOM_{TPA}}$ is nearly constant for the W1-PCW, with a value slightly above the silicon material $\mathrm{FOM_{TPA}}$ of 0.38. This result is consistent with the fact that the overlap between the mode field and the nonlinear material filling the holes is then weak. On the contrary, we clearly observe an increase of $\mathrm{FOM_{TPA}}$ for the two slow light slotted waveguide geometries, with a saturation effect for large group index values. We notice that the increase of $\mathrm{FOM_{TPA}}$ from $n_G = 10$ to $n_G = 50$ can be large. A precise data inspection shows that the enhancement is around +33.4% and +72.7% in the NS-PCW and WS-PCW geometries, respectively. Beyond these precise values that may slightly depend on the precise parameters of the investigated waveguides, we arrive to the conclusion that silicon slotted slow light waveguides exhibit a decreasing relative effect of TPA for increasing slowing-down factors. This result brings the interesting information that operating in the slow light regime with hybrid waveguides does not spoil the Kerr/TPA balance but on the contrary contributes to improving the nonlinear waveguide performance.

## 3. CONCLUSION

To conclude, we show in this paper that properly filled silicon SPCWs do not have the same behavior as standard W1 ones with respect to the influence of slow light on the TPA process at telecommunication wavelengths. Both narrow and wide slot PCWs, operating on the two slot PCW modes (W1-like and true-slot modes, respectively), are characterized by a mode field concentration in the slot for increasing slow-down factors. These results show that the hybrid platform made of nonmembrane slow light slotted silicon waveguides filled with nonlinear low-index materials can efficiently rely on slow light effects for on-chip data processing. The relatively free-carrier penalty indeed tends to decrease with increasing slow down factors.

**Funding.** Agence Nationale de la Recherche (ANR) (POSISLOT)

**Acknowledgment.** We would like to warmly acknowledge Dr. Nicolas Dubreuil for fruitful discussions.

## REFERENCES

1. L. Vivien and L. Pavesi, *Handbook of Silicon Photonics* (CRC, 2013).
2. I.-W. Hsieh, X. Chen, X. Liu, J. I. Dadap, N. C. Panoiu, C.-Y. Chou, F. Xia, W. M. Green, Y. A. Vlasov, and R. M. Osgood, "Supercontinuum generation in silicon photonic wires," Opt. Express **15**, 15242–15249 (2007).
3. R. Osgood, N. Panoiu, J. Dadap, X. Liu, X. Chen, J. Hsieh, and Y. Vlasov, "Engineering nonlinearities in nanoscale optical systems: physics and applications in dispersion-engineered silicon nanophotonic wires," Adv. Opt. Photon. **1**, 162–235 (2009).
4. C. Monat, B. Corcoran, D. Pudo, M. Ebnali-Heidari, C. Grillet, M. D. Pelusi, and T. F. Krauss, "Slow light enhanced nonlinear optics in silicon photonic crystal waveguides," IEEE J. Sel. Top. Quantum Electron. **16**, 344–356 (2010).
5. Y. Okawachi, K. Saha, J. S. Levy, Y. H. Wen, M. Lipson, and A. L. Gaeta, "Octave-spanning frequency comb generation in a silicon nitride chip," Opt. Lett. **36**, 3398–3400 (2011).
6. Q. Lin, O. J. Painter, and G. P. Agrawal, "Nonlinear optical phenomena in silicon waveguides: modeling and applications," Opt. Express **15**, 16604–16644 (2007).
7. W. Zhang, S. Serna, N. Dubreuil, and E. Cassan, "Nonlinear optimization of slot Si waveguides: TPA minimization with $\mathrm{FOM_{TPA}}$ up to 4.25," Opt. Lett. **40**, 1212–1215 (2015).
8. A. Di Falco, L. O'Faolain, and T. F. Krauss, "Photonic crystal slotted slab waveguides," Photon. Nanostruct. **6**, 38–41 (2008).
9. C. Caer, X. Le Roux, S. Serna, W. Zhang, L. Vivien, and E. Cassan, "Large group-index bandwidth product empty core slow light photonic crystal waveguides for hybrid silicon photonics," Front. Optoelectron. **7**, 376–384 (2014).
10. C. Caer, X. Le Roux, and E. Cassan, "Enhanced localization of light in slow wave slot photonic crystal waveguides," Opt. Lett. **37**, 3660–3662 (2012).
11. T. Krauss, "Slow light in photonic crystal waveguides," J. Phys. D **40**, 2666–2670 (2007).
12. J. F. McMillan, M. Yu, D.-L. Kwong, and C. W. Wong, "Observation of four-wave mixing in slow-light silicon photonic crystal waveguides," Opt. Express **18**, 15484–15497 (2010).
13. C. A. Barrios, "High-performance all-optical silicon microswitch," Electron. Lett. **40**, 862–863 (2004).
14. M. Asobe, I. Yokohama, T. Kaino, S. Tomaru, and T. Kurihara, "Nonlinear absorption and refraction in an organic dye functionalized main chain polymer waveguide in the 1.5 μm wavelength region," Appl. Phys. Lett. **67**, 891–893 (1995).
15. C. Koos, P. Vorreau, T. Vallaitis, P. Dumon, W. Bogaerts, R. Baets, B. Esembeson, I. Biaggio, T. Michinobu, F. Diederich, W. Freude, and J. Leuthold, "All-optical high-speed signal processing with silicon-organic hybrid slot waveguides," Nat. Photonics **3**, 216–219 (2009).
16. S. G. Johnson and J. D. Joannopoulos, "Block-iterative frequency-domain methods for Maxwell's equations in a plane-wave basis," Opt. Express **8**, 173–190 (2001).
17. S. Hughes, L. Ramunno, J. F. Young, and J. E. Sipe, "extrinsic optical scattering loss in photonic crystal waveguides: role of fabrication disorder and photon group velocity," Phys. Rev. Lett. **94**, 033903 (2005).
18. N. C. Panoiu, J. F. McMillan, and C. W. Wong, "Theoretical analysis of pulse dynamics in silicon photonic crystal wire waveguides," IEEE J. Sel. Top. Quantum Electron. **16**, 257–266 (2010).
19. S. Lavdas and N. C. Panoiu, "Theory of pulsed four-wave mixing in one-dimensional silicon photonic crystal slab waveguides," Phys. Rev. B **93**, 115435 (2016).

210.72.9.236 {ts '2016-11-21 01:12:44'}